

CDMA-based Analog Network Coding through Interference Cancellation for Underwater Acoustic Sensor Networks

Hovannes Kulhandjian[†], Tommaso Melodia[†], and Dimitrios Koutsonikolas[‡]

[†]Department of Electrical Engineering

[‡]Department of Computer Science and Engineering
State University of New York at Buffalo, Buffalo, New York 14260
Email: {hkk2, tmelodia, dimitrio}@buffalo.edu

ABSTRACT

The performance of multi-hop underwater acoustic network is known to be limited by the long propagation delays and by the limited bandwidth of the underwater acoustic (UW-A) channel. Recent work on analog network coding (ANC) has shown that significant throughput gains can be achieved in multi-hop wireless networks. However, implementing ANC for UW-A communications is very challenging as the UW-A channel is severely affected by multipath. In this paper, we propose CE-CDMA, a collision-enabling direct-sequence code-division multiple-access scheme for multi-hop underwater acoustic sensor networks (UW-ASNs). In CE-CDMA two nodes, separated by two hops, are assigned the same code-division channel (i.e., spreading code) to communicate concurrently. The transmission of packets by the two nodes will therefore collide at the intermediate (relay) node. However, we show that by exploiting *a priori* information, i.e., the interfered packet previously received from one of the nodes, and an adaptive RAKE receiver that jointly estimates the two multipath-affected channels, the relay node can cancel the interference before decoding the packet of interest. Experiments demonstrate that for a 1–2dB tradeoff in signal-to-noise ratio (SNR) the proposed scheme can potentially improve the channel utilization of a unidirectional multi-hop linear network by up to 50%. We also outline the basic functionalities of a MAC protocol (CE-MAC) designed to support the proposed scheme.

1. INTRODUCTION

Underwater sensor networks have attracted considerable attention recently, due to increasing interest in many military and commercial applications [2, 15, 24, 12]. Although radio frequency (RF) electromagnetic and optical waves are the dominant physical communication carriers in terrestrial wireless communications, in water they are severely affected by high attenuation and scattering, respectively. Acoustic communication is therefore the transmission technology of choice for underwater networked systems [15].

The UW-A channel is known to suffer from limited band-

width and spectral efficiency. Recently proposed physical layer network coding (PNC) [28] and analog network coding (ANC) [10] schemes have demonstrated significant improvements in spectral efficiency and throughput gains under several network scenarios. The basic idea of PNC and ANC is to better utilize the wireless bandwidth by allowing concurrent transmissions of signals over the wireless medium so that they intentionally interfere with each other. The receiver, having heard the interfered signal from prior transmissions, will cancel the interference before decoding the desired information.

The objective of this paper is to explore the idea of ANC, which is essentially a form of linear self-interference cancellation with the use of *a priori* information [3], in multi-hop UW-ASNs. The idea of linear self-interference cancellation was first introduced in [8] and over the years it has evolved in different forms [13, 20, 19, 5, 3].

Unlike in terrestrial wireless communications, in UW-A communications multipath is prevalent. Therefore, designing a receiver tailored for ANC that extracts the information of interest from the two interfered signals in severely affected multipath channels is very challenging. To the best of our knowledge, no prior work has explored ANC in such channels; particularly in *shallow water* UW-A channels.

We consider a code-division multiple-access (CDMA) scheme. CDMA is considered one of the most promising physical layer and multiple access techniques for UW-ASNs [18], since it is robust to frequency-selective fading and can compensate for the effect of multipath through RAKE receivers [24].

We therefore introduce CE-CDMA, a collision-enabling direct-sequence code-division multiple-access scheme for multi-hop UW-ASNs. We develop a CDMA-based scheme to cancel interference by using *a priori* information and jointly estimating the two multipath channels. We outline the basic functionalities of a MAC protocol (CE-MAC) that leverages the proposed CE-CDMA scheme. Simulations and testbed experiments are conducted to evaluate the performance of the proposed scheme in terms of bit error rate (BER) and packet error rate (PER) and are compared to conventional DS-CDMA. Performance evaluation results reveal that the proposed scheme performs close to conventional DS-CDMA in terms of BER and PER for a given SNR. Moreover, at the price of 1–2dB increase in SNR, it can achieve a throughput gain of up to 50% for a target BER level.

The rest of this paper is organized as follows. We first introduce the collision-enabling CDMA scheme in Section 2. In Section 3, we describe the system model of a DS-CDMA scheme. Detailed discussions on joint channel estimation and the proposed receiver design are presented in Sections 4

Permission to make digital or hard copies of all or part of this work for personal or classroom use is granted without fee provided that copies are not made or distributed for profit or commercial advantage and that copies bear this notice and the full citation on the first page. To copy otherwise, to republish, to post on servers or to redistribute to lists, requires prior specific permission and/or a fee.

WUWNet'12, Nov. 5–6, 2012 Los Angeles, California, USA.
Copyright 2012 ACM 978-1-4503-1773-3/12/11 ... \$15.00.

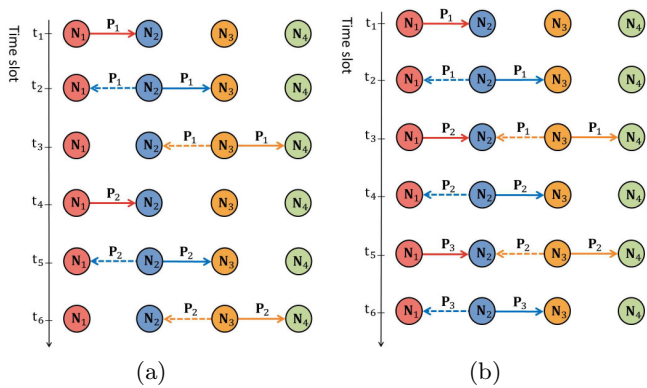


Figure 1: Four-node chain network topology: (a) Conventional CDMA scheduling, (b) Collision-enabling CDMA scheduling.

and 5 respectively. In Section 6, we present the basic design principles behind CE-MAC, while in Section 7, we evaluate the proposed scheme. Finally, in Section 8, we conclude and provide future extensions to the proposed work.

Notation: The following notation is used throughout the paper. Boldface lower-case letters indicate column vectors, boldface upper-case letters indicate matrices, \mathbf{x}^H denotes the Hermitian of vector \mathbf{x} , \mathbf{I} is the identity matrix, $\text{tr}\{\mathbf{X}\}$ represents the trace of a matrix \mathbf{X} , $\mathbb{E}\{\cdot\}$ represents statistical expectation, $\|\cdot\|$ is the Euclidean norm of a vector, $\text{Re}(\cdot)$ denotes the real part of a complex valued vector, $\text{sgn}(\cdot)$ denotes zero-threshold quantization and \oplus denotes bitwise modulo 2 addition.

2. MOTIVATION

In this section, we illustrate the idea of collision-enabling DS-CDMA communications in a four-node linear network topology. In an UW-ASN, utilizing a conventional multi-user DS-CDMA scheme, each node is assigned a binary spreading code of length L to access a common (in time and frequency) communication channel.

Unidirectional multi-hop linear topology. We consider a wireless multi-hop linear network topology, shown in Fig. 1(a). In this scenario, a source, denoted by N_1 , would like to transmit packets P_1, P_2 , etc., through multi-hop routing, to the destination, N_4 , using a unique spreading code previously assigned to it. It takes three times slots to convey a packet from the source to the destination. The solid line indicates the scheduled transmissions, while the dashed line is the interference generated due to the broadcast nature of wireless transmission. When packet P_1 is being forwarded by N_3 in time slot t_3 , N_1 should not use the same spreading code to transmit P_2 , since N_3 's transmission may cause interference to N_2 .

The average throughput and end-to-end delay of this network will be improved if we allow concurrent transmissions by two nodes located two hops away, eg., N_1 and N_3 . Concurrent transmissions will allow N_1 to transmit P_2 , while N_3 is forwarding P_1 to the destination, N_4 , in time slot t_3 using the same spreading code. The two packets, P_1 and P_2 will interfere with each other at N_2 . However, using *a priori* information, P_1 , from the time slot t_2 , N_2 will cancel the interference generated by N_3 , before decoding P_2 and forwarding it to N_3 in the next time slot. The proposed collision-enabling CDMA scheduling scheme is shown in Fig. 1(b). Under this scheduling scheme the wireless chan-

nel is further exploited, since no additional time slot is required to transmit the packet, P_2 , from N_1 to N_2 . Utilizing the collision-enabling scheduling scheme on average only two time slots are needed to transmit a packet from source to destination. The performance gain of scheduling scheme can be expressed by the transmission efficiency, defined in [5] as the ratio of the time taken for the transmission of P packets under the conventional scheduling scheme and the scheduling scheme employing overlapped transmissions, respectively. The transmission efficiency, Γ_4 , for the four-node scenario presented above is given by

$$\Gamma_4 = \frac{3P}{2(P-1)+3} \approx \frac{3}{2}, P \gg 1, \quad (1)$$

where P is the total number of packets transmitted by N_1 . Equivalently, for a linear network topology with $N(N \geq 4)$ nodes, as shown in [5], the same gain is achieved for $P \gg 1$.

We observe that utilizing the proposed scheme in a multi-hop chain topology has the potential to improve the efficiency of the unidirectional linear network by up to 50% over the conventional scheduling scheme.

3. SYSTEM MODEL

In this section, we discuss the system model of a DS-CDMA scheme. We consider a DS-CDMA system with K users transmitting asynchronously over a frequency-selective fading channel. The baseband signal transmitted by the k^{th} user is

$$u_k(t) = \sum_i b_k(i) \sqrt{E_k} s_k(t - iT), \quad (2)$$

where $b_k(i) \in \{-1, 1\}$ denotes the i^{th} element of the information-bearing sequence, E_k denotes the transmitted energy per bit, $s_k(t)$ is the normalized spreading waveform given by

$$s_k(t) = \frac{1}{L} \sum_{l=1}^L d_k(l) p(t - lT_c). \quad (3)$$

In (3), without loss of generality, we assume binary phase shift keying (BPSK) is applied such that $d_k(l) \in \{-1, 1\}$ is the l^{th} transmitted chip of the k^{th} user's spreading sequence, $p(t)$ is the chip pulse shape and $L = T/T_c$ is the processing gain, where T_c is the chip period and T is the information bit duration [9].

The total baseband received signal at the receiver is

$$r(t) = \sum_i \sum_{k=1}^K b_k(i) \sum_{m=1}^M h_{k,m} \sqrt{E_k} s_k(t - iT - \frac{m}{B} - \tau_k) + n(t), \quad (4)$$

where $h_{k,m}$ is the channel coefficient corresponding to the k^{th} user due to multipath branch m of the frequency-selective slowly fading channel. The channel coefficients are modeled as independent zero-mean complex Gaussian random variables that remain constant within a bit interval, $n(t)$ is a zero-mean complex additive white Gaussian noise (AWGN) and τ_k is the relative delay of the user k . Multipath spread in shallow water acoustic channel is in the order of a few tens of chip intervals T_c [25] and since the signal is bandlimited to $B = 1/T_c$, the tap delay line channel mode has taps spaced at chip intervals T_c . Spreading codes of length higher than the multipath spread are selected.

After chip-matched filtering and sampling at the chip rate the chip synchronous equivalent received signal of vector

composed of $L + M - 1$ samples is given by

$$\begin{aligned} \mathbf{r}(i) = & \sum_{k=1}^K b_k(i) \sum_{m=1}^M h_{k,m} \sqrt{E_k} \mathbf{s}_{k,m}^0 + \\ & + \sum_{k=1}^K b_k(i+1) \sum_{m=1}^M h_{k,m} \sqrt{E_k} \mathbf{s}_{k,m}^+ + \\ & + \sum_{k=1}^K b_k(i-1) \sum_{m=1}^M h_{k,m} \sqrt{E_k} \mathbf{s}_{k,m}^- + \mathbf{n}(i). \end{aligned} \quad (5)$$

The received signal incorporates all the delayed chips carrying the information bit of interest. The vectors $\mathbf{s}_{k,m}^0$, $\mathbf{s}_{k,m}^+$ and $\mathbf{s}_{k,m}^-$ correspond to the spreading code of user k due to multipath branch m generated by transmitted bits $b(i)$, $b(i+1)$ and $b(i-1)$, respectively, while \mathbf{n} is assumed to be zero-mean complex AWGN with autocorrelation matrix $E\{\mathbf{nn}^H\} = \sigma^2 \mathbf{I}_{(L+M-1) \times (L+M-1)}$ with the variance σ^2 [9]. Having explained the system model of the DS-CDMA receiver, in our scheme, we discuss the details behind our joint channel estimation algorithm and receiver design next.

4. JOINT CHANNEL ESTIMATION

Due to the highly-frequency selective distortion caused by multipath propagation in UW-A channel, it is essential to estimate the channel state information (CSI) periodically. To capture the frequency-selectivity of the UW-A channel adaptively, we develop an algorithm that jointly estimates the CSI of the two users through pilot supervision. We utilize a set of N_p pilot bits inserted in each packet distanced less than the coherence time, T_{CT} , of the channel to jointly estimate both channels. We then design a DS-CDMA receiver, discussed in Section 5, that cancels the interference caused by the node utilizing the same spreading code, before decoding the information of interest.

In our model we describe DS-CDMA system with $K = 2$ users, (Alice and Bob), both utilizing the same spreading code to access the channel. We consider a linear network topology shown in Fig. 1(b), in which Alice and Bob have packets to transmit to their adjacent relay node. Alice can be considered N_1 , while Bob N_3 . Alice would like to transmit P_2 to N_2 , while Bob needs to convey P_1 to N_4 . After the relay node, N_2 , receives the interfered data packets transmitted by Alice and Bob, using the pilot bits, it will first estimate the CSIs from Alice-to-relay and Bob-to-relay, before it decodes the packet of interest to be relayed to the next node, N_3 , in the next transmission round. The supervised information bits transmitted by Alice and Bob are

$$\mathbf{x}_A(i) = b_A(i) \sqrt{E_A} \mathbf{s}, \quad (6)$$

$$\mathbf{x}_B(i) = b_B(i) \sqrt{E_B} \mathbf{s}, \quad (7)$$

where \mathbf{s} denotes the spreading codes used by Alice and Bob, $b_A(i)$, $b_B(i) \in \{-1, 1\}$ are i^{th} pilot bits transmitted by Alice and Bob, respectively, where $i = 1, 2, \dots, N_p$.

To simplify the problem formulation, we assume the transmission is chip-level synchronized and the packets transmitted by Alice and Bob arrive at the relay simultaneously. The proposed scheme relaxes the strict synchronous arrival of the two packets at the relay, which is difficult to achieve due to long propagation delays in UW-A channel. The details on symbol synchronization for chip matched filtering and multipath spread estimation are discussed in Section 6.

After chip-matched filtering and sampling at the chip rate, the received signal (the i^{th} bits) is denoted by

$$\mathbf{r}(i) = \sqrt{E_A} \mathbf{S}_A(i) \mathbf{h}_A + \sqrt{E_B} \mathbf{S}_B(i) \mathbf{h}_B + \mathbf{n}(i), \quad (8)$$

where

$$\mathbf{h}_A = [h_{A1}, h_{A2}, \dots, h_{AM}]^H, \quad (9)$$

and

$$\mathbf{h}_B = [h_{B1}, h_{B2}, \dots, h_{BJ}]^H, \quad (10)$$

are multipath channel coefficients of Alice-to-relay and Bob-to-relay of lengths M and J , respectively. Without loss of generality, we assume $M = J$, where each component is modeled as complex additive white Gaussian variable with zero-mean and variance of one, \mathbf{n} is assumed to be zero-mean complex AWGN with autocorrelation matrix $E\{\mathbf{nn}^H\} = \sigma^2 \mathbf{I}_{(L+M-1) \times (L+M-1)}$, and

$$\mathbf{S}_A(i) = \mathbf{S}_A^0(i) + \mathbf{S}_A^+(i) + \mathbf{S}_A^-(i), \quad (11)$$

$$\mathbf{S}_B(i) = \mathbf{S}_B^0(i) + \mathbf{S}_B^+(i) + \mathbf{S}_B^-(i), \quad (12)$$

where

$$\mathbf{S}_k^0(i) = b_k(i) \begin{bmatrix} s_1 & 0 & \dots & 0 \\ \vdots & s_1 & \ddots & \vdots \\ s_L & \vdots & \ddots & 0 \\ 0 & s_L & & s_1 \\ \vdots & \vdots & \ddots & \vdots \\ \vdots & \vdots & \ddots & \vdots \\ 0 & 0 & \dots & s_L \end{bmatrix}_{(L+M-1) \times M}, \quad (13)$$

$$\mathbf{S}_k^+(i) = b_k(i+1) \begin{bmatrix} 0 & \dots & 0 & 0 \\ \vdots & \ddots & \vdots & \vdots \\ 0 & 0 & 0 & 0 \\ s_1 & \ddots & \vdots & 0 \\ \vdots & \ddots & 0 & \vdots \\ s_{M-1} & \dots & s_1 & 0 \end{bmatrix}_{(L+M-1) \times M}, \quad (14)$$

$$\mathbf{S}_k^-(i) = b_k(i-1) \begin{bmatrix} 0 & s_L & \dots & s_{L-M+1} \\ \vdots & 0 & \ddots & \vdots \\ 0 & \vdots & \ddots & s_L \\ 0 & 0 & & 0 \\ \vdots & \vdots & \ddots & \vdots \\ 0 & 0 & \dots & 0 \end{bmatrix}_{(L+M-1) \times M}. \quad (15)$$

The matrices $\mathbf{S}_k^0(i)$, $\mathbf{S}_k^+(i)$ and $\mathbf{S}_k^-(i)$ correspond to the spreading code matrices generated due to the transmission of bits $b(i)$, $b(i+1)$ and $b(i-1)$, respectively, by user $k \in \{A, B\}$, Alice or Bob in this case. Let us define

$$\mathbf{S}_{AB}(i) \triangleq \begin{bmatrix} \sqrt{E_A} \mathbf{S}_A(i), & \sqrt{E_B} \mathbf{S}_B(i) \end{bmatrix}_{(L+M-1) \times 2M} \quad (16)$$

and

$$\mathbf{h}_{AB} \triangleq \begin{bmatrix} \mathbf{h}_A \\ \mathbf{h}_B \end{bmatrix}_{2M \times 1}. \quad (17)$$

We may rewrite (8) into a more compact form as

$$\mathbf{r}(i) = \mathbf{S}_{AB}(i) \mathbf{h}_{AB} + \mathbf{n}(i). \quad (18)$$

Before jointly estimating the channel coefficients, \mathbf{h}_A and \mathbf{h}_B , we first define the pseudo-inverse of $\mathbf{S}_{AB}(i)$ for $(L+M-$

1) $> 2M$ using the Moore-Penrose pseudo-inverse formula as

$$\mathbf{S}_{AB}(i)^\dagger \triangleq \left(\mathbf{S}_{AB}(i)^H \mathbf{S}_{AB}(i) \right)^{-1} \mathbf{S}_{AB}(i)^H, \quad (19)$$

since $\mathbf{S}_{AB}(i)$ might not be a square matrix.

We can obtain the least square (LS) estimate of \mathbf{h}_{AB} by minimizing the following squared error quantity

$$\hat{\mathbf{h}}_{AB} = \arg \min_{\mathbf{h}_{AB}} \|\mathbf{r}(i) - \mathbf{S}_{AB}(i)\mathbf{h}_{AB}\|^2. \quad (20)$$

Since the channel noise is assumed to be complex AWGN, the solution of (20) can be estimated by sample averaging over a data record of N_p pilot bits as

$$\hat{\mathbf{h}}_{AB} = \frac{1}{N_p} \sum_{i=1}^{N_p} \mathbf{S}_{AB}(i)^\dagger \mathbf{r}(i). \quad (21)$$

The estimates given by the LS (21) are simply scaled correlations between the received signal and training sequences.

We can obtain an accurate estimate of \mathbf{h}_{AB} *if and only if* (16) is of full rank. This condition is satisfied if (16) contains $2M$ independent vectors. In this work, we use columns of a Sylvester-Hadamard matrix, \mathbf{H}_L , of order $L = 2^n$, $n = 2, 3, \dots$, as our spreading code. The Sylvester-Hadamard matrix has good autocorrelation and cross-correlation properties. Each row or column of a \mathbf{H}_L is orthogonal to each other. For a spreading code extracted from a \mathbf{H}_L of order $L = 4$, the above condition cannot be satisfied for $M = 3$, hence a spreading code length of $L = 8$ or longer should be used in this case.

The noisy nature of the acoustic channel results in SNR degradation in joint channel estimation, an approximation of which is given in [23] as

$$d_{ce}/dB = 10 \cdot \log_{10} \left[1 + \text{tr} \left\{ \left(\mathbf{S}_{AB}(i)^H \mathbf{S}_{AB}(i) \right)^{-1} \right\} \right]. \quad (22)$$

Therefore, it is important to select the training sequences for both nodes with very low cross-correlation properties to minimize the noise enhancement. Accordingly, we utilize two sequences of pilot bits extracted again from a \mathbf{H}_L , of order $L = 2^n$, $n = 4, 5, \dots$.

The CSI from Alice-to-relay and Bob-to-relay are found as follows

$$\hat{\mathbf{h}}_{\mathbf{A}} = [\mathbf{I}_{M \times M} \mathbf{0}_{M \times M}] \hat{\mathbf{h}}_{\mathbf{AB}}, \quad (23)$$

$$\hat{\mathbf{h}}_{\mathbf{B}} = [\mathbf{0}_{M \times M} \mathbf{I}_{M \times M}] \hat{\mathbf{h}}_{\mathbf{AB}}, \quad (24)$$

where $\mathbf{I}_{M \times M}$ and $\mathbf{0}_{M \times M}$ are $M \times M$ identity and zero matrices respectively.

The mean square error (MSE) per real channel coefficient $\hat{\mathbf{h}}_{\mathbf{A}}$, is given by

$$MSE = \mathbb{E} \left\{ \|\hat{\mathbf{h}}_{\mathbf{A}} - \mathbf{h}_{\mathbf{A}}\|^2 \right\}. \quad (25)$$

We evaluate the MSE of channel estimates $\hat{\mathbf{h}}_{\mathbf{A}}$ and $\hat{\mathbf{h}}_{\mathbf{B}}$ for various SNR values in Section 7.

The system model for the proposed CE-CDMA joint channel estimation is shown in Fig. 2.

5. RECEIVER DESIGN

In this section, we design the CE-CDMA receiver that cancels the interference caused by the secondary user utilizing the same spreading code to access the channel. To

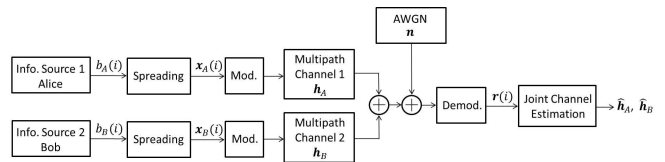


Figure 2: CE-CDMA system model with joint channel estimation.

decode the information bits, we use the estimated CSIs, $\hat{\mathbf{h}}_{\mathbf{A}}$, $\hat{\mathbf{h}}_{\mathbf{B}}$, and design a RAKE-matched-filter that decides on the transmitted bit of the user of interest (Alice) based on the sum of the individual M path-correlator outputs; which can be equivalently characterized by the normalized static $(L + M - 1)$ -tap FIR filter given by

$$\mathbf{w}_{RAKE_{MF}} = \frac{\mathbf{S}_{MF} \hat{\mathbf{h}}_{\mathbf{A}}}{(\mathbf{S}_{MF} \hat{\mathbf{h}}_{\mathbf{A}})^H (\mathbf{S}_{MF} \hat{\mathbf{h}}_{\mathbf{A}})}, \quad (26)$$

where

$$\mathbf{S}_{MF} = \begin{bmatrix} s_1 & 0 & \dots & 0 \\ \vdots & s_1 & & \vdots \\ & \vdots & \ddots & 0 \\ s_L & \vdots & & 0 \\ 0 & s_L & & s_1 \\ \vdots & \vdots & \ddots & \vdots \\ 0 & 0 & \dots & s_L \end{bmatrix}_{(L+M-1) \times M}, \quad (27)$$

represents the M path-correlator outputs, which can be constructed knowing the number of multipaths, M .

Before decoding the information bits, we first cancel the inter-symbol-interference (ISI) resulting from the previously decoded bits. Moreover, we cancel the estimated interfered data bits from Bob and, employing the RAKE-matched-filter proposed in (26), the information bits ($j = 1, 2, \dots$) of the user of interest (Alice) are decoded as follows

$$\hat{b}_A(j) = \text{sgn} \left(\text{Re} \left[\mathbf{w}_{RAKE_{MF}}^H \left(\mathbf{r}(j) - \mathbf{S}_B(j) \hat{\mathbf{h}}_{\mathbf{B}} - \mathbf{S}_A^-(j) \hat{\mathbf{h}}_{\mathbf{A}} \right) \right] \right), \quad (28)$$

where $\mathbf{S}_A^-(j) \hat{\mathbf{h}}_{\mathbf{A}}$ is the ISI of the previously decoded bit and $\mathbf{S}_B(j) \hat{\mathbf{h}}_{\mathbf{B}}$ is the estimate of the interfered data bit. We assume the previous bit is correctly decoded. The receiver design for the proposed CE-CDMA scheme is shown in Fig. 3.

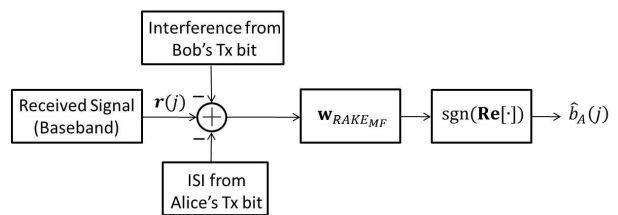


Figure 3: Receiver design for CE-CDMA.

6. CE-MAC BASIC DESIGN PRINCIPLES

In this section, we outline the basic functionalities of a MAC protocol (CE-MAC) designed to leverage the proposed CE-CDMA scheme. Detailed evaluation of CE-MAC is left for future work.

The majority of existing UW-A MAC protocols [22, 7, 6, 16, 17] utilize a handshaking scheme by transmitting

small RTS/CTS packets to establish a connection between a source and a destination before the actual data transmission. In addition to that, usually, a separate ACK is sent to acknowledge the reception of the data. Due to the high propagation delay in UW-A channels, we avoid implementing a handshaking mechanism as well as separate ACK transmission.

In CE-MAC, after a node transmits a packet, it cannot transmit another packet before it overhears the next hop forwarding that packet. This establishes an implicit slot-based transmission but without any explicit synchronization algorithm [21]. CE-MAC is based on the CE-CDMA scheme discussed in Section 3, in which, all nodes are informed of and utilize a common spreading code for header, trailer, and the first set of pilot bits transmission. For the payload and the intermediate pilot bits, each source utilizes a unique spreading code, the information of which is included in the header/trailer of the packet before transmission.

Packet Structure. Before we illustrate the functionalities of the proposed MAC, we present the packet structure shown in Fig. 4. Each packet is of the same length and is comprised of a preamble, a guard-band, a pilot sequence followed by a header, a sequence of payload fragments separated by intermediate pilot bits, a trailer, a guard-band and a postamble. The preamble and postamble are identical chirp signals of duration 100ms sweeping the bandwidth from 10 Hz to 2.6 kHz. They are used for channel probing, symbol synchronization for chip matched filtering and multipath delay spread estimation. The guard-band is a pause duration longer than the maximum expected multipath delay spread and is used to prevent the preamble/postamble from interfering with the header/trailer. In shallow water communications the multipath delay spread is in the order of 10ms [14] and a guard-band of 50ms is often selected [26]. The pilot bits, as discussed in Section 4, are used for channel estimation. The additional postamble, guard-band, and trailer are introduced in order not to restrict which packet has to arrive at the receiving node first, to avoid header collision. In UW-A communication it is very difficult to guarantee synchronization as an UW-A channel experiences high and variable propagation delays. In case packets arrive synchronously and the relay node is not able to decode the header/trailer, the packets are dropped and, after a timeout period, they are retransmitted.

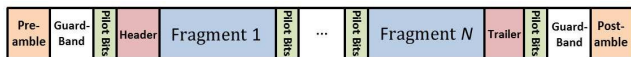


Figure 4: Packet structure.

Packet Header and Trailer Structure. The packet's header and trailer, shown in Fig. 5, contain information on the spreading code to use to decode the payload, sequence numbers of payload fragments, cumulative acknowledgment, and transmitter and receiver node ID numbers.

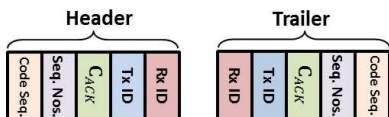


Figure 5: Packet header and trailer.

Packet Fragmentation. Utilizing the proposed scheme, it is desirable to increase the length of the payload to reduce the overhead of preamble/postamble, header/trailer,

and guard-band for each data packet. The longer the payload size the higher the throughput [4]. However, increasing the payload size will result in higher PER and as a consequence will increase the number of retransmissions, which in turn will decrease the achievable throughput. In [4], Basagni et al. have shown that fragmenting a long packet helps to reduce the number of retransmissions.

Consequently, the payload is divided into N fragments and at the end of each fragment a cyclic redundancy check (CRC) is appended. The CRC is used for detecting the erroneous fragments and retransmit only those fragments that cannot be correctly decoded, using a selective repeat automatic repeat-request (ARQ) protocol.

Moreover, to avoid wasting bandwidth by transmitting a separate ACK, we utilize instead a cumulative acknowledgment (C_{ACK}), which is included in the header/trailer of the newly generated packet to be relayed to the next hop, to acknowledge the reception of the correctly received fragments. The C_{ACK} is similar to the one introduced in [11] and contains the transmitter's MAC address followed by initial fragment sequence number and a bitmap of length N_{MAX} bits to indicate the correctly received and missing fragments. N_{MAX} corresponds to the maximum number of pending unacknowledged fragments. As an example, a $C_{ACK} = \{N_2, 7, 111110\}$ means node N_2 acknowledges correctly received fragments from 7 to 11 and is missing fragment 12. The fragment sequence numbers in the header/trailer of the packet are of similar format to make them more compact. Due to the broadcast nature of the wireless acoustic channel, Alice will likely receive and decode the transmitted packet's header/trailer and retrieve the C_{ACK} information. In case Alice does not overhear the C_{ACK} within a timeout period, T_{TA} , which is slightly longer than the link round-trip time (RTT), she will retransmit the same packet in the next transmission round. We assume each node has a reasonably large buffer size to store the correctly received fragments.

Functionalities of CE-MAC. To illustrate the functionalities of the proposed CE-MAC protocol, we refer to the timing diagram shown in Fig. 6. We assume all nodes are equidistant and within one broadcast-hop range from each other. Alice, N_1 , would like to transmit packets P_1 , P_2 , etc. to the destination node N_4 . Initially, Alice transmits P_1 , containing three fragments shown in Fig. 7(a), to the relay node, N_2 . After a propagation plus transmission delay ($T_{prop.} + T_{tran.}$), N_2 receives the packet and tries to decode it within a processing time ($T_{proc.}$). If some of the fragments cannot be correctly decoded, assume fragment 2, N_2 will ask for retransmissions of this fragment in the next transmission round from Alice. The information of the requested fragment will be included in the C_{ACK} of the header/trailer of the newly generated packet to be relayed to the next hop. In this case, when Alice receives $C_{ACK} = \{N_2, 1, 10100\}$, she is informed that node N_2 received fragments 1 and 3 correctly and is requesting fragment 2. Notice that the number of bits allocated for N_{MAX} is on purpose selected to be longer than N to allow acknowledgement of fragments received from different transmission rounds. In the next transmission round, N_2 forwards P_1' , shown in Fig. 7(b), to N_3 . Note that P_1' might not be the original packet, P_1 , since P_1' contains the fragments requested by the upstream node, N_3 , if any, followed by the correctly decoded fragments from the downstream node, Alice. If there are extra fragment slots left, N_2 will include a network coded version of the first pair of fragments to be transmitted to N_3 in those

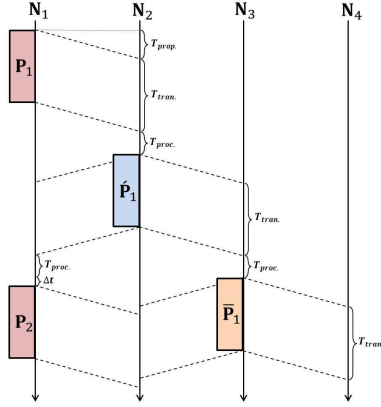


Figure 6: CE-MAC timing diagram.

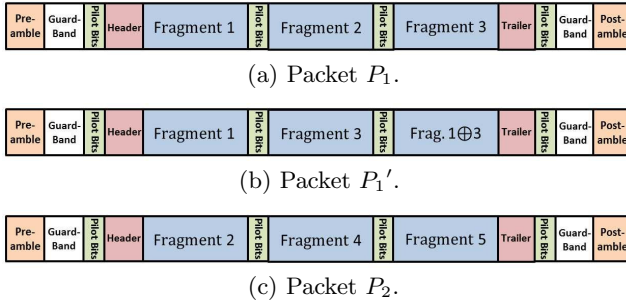


Figure 7: Packets P_1 , P_1' and P_2 .

empty slots. The additional mixed fragments are intended to increase N_3 's success rate in decoding the fragments of interest correctly. In this example, N_2 will first place the correctly received fragments 1 and 3, and for the remaining empty fragment slot it will include a mixed fragment (fragment 1 \oplus fragment 3). By receiving any two combinations of fragments correctly, N_3 will be able to decode the two fragments of interest. If we assume N_3 received fragments 1 and the mixed fragment, (fragment 1 \oplus fragment 3), correctly, to decode the fragment 3, it will perform bitwise modulo-2 addition of the two correctly decoded fragments. When Alice receives P_1' , she is notified through C_{ACK} about the fragments requested by N_2 . In the next transmission round, N_3 transmits \bar{P}_1 to the destination, while Alice backs off for a small random time, Δt , before transmitting P_2 to N_2 . P_2 , shown in Fig. 7(c), contains the missing fragment 2 requested from N_2 and a new set of fragments. Backing off by Δt will help to avoid simultaneous arrival of the two packets at N_2 , as the header/trailer from each packet may interfere with each other. The rest of the packets are transmitted in a similar way with the intention to encourage collision of the two packets at the intermediate relay node whenever opportunities arise.

The proposed CE-MAC is resilient to the *hidden terminal problem*, as it allows nodes two hops away to transmit packets to their adjacent neighboring nodes concurrently, without worrying about packets colliding at the intermediate node.

7. PERFORMANCE EVALUATION

In this section, using simulations and testbed experiments, we evaluate the performance of CE-CDMA scheme and compare it with the conventional DS-CDMA in terms of average

BER and PER. The average MSE of the joint channel estimation is also studied.

7.1 Simulation Results

Simulations of the proposed CE-CDMA scheme were performed in Matlab. The Alice and Bob topology, discussed in Section 4, was implemented in which both nodes concurrently transmit their packets, which collide at the relay node. Both channels, Alice-to-relay and Bob-to-relay, are modeled as Rayleigh fading in which the multipath channel coefficients are considered as independent zero-mean complex Gaussian random variables of variance one, and the number of multipaths, M and J , are randomly selected. The relay node estimates the CSIs from the two nodes and cancels the interference, Bob's packet, before decoding the information of interest, Alice's packet. The fragment size is determined based on the average coherence time of a shallow water acoustic channel, which is in the order of a few seconds for a transmission frequency of 10 kHz [27]. Accordingly, a fragment size of 125 Bytes is selected. Unless otherwise stated, the parameters used for simulations are payload size = 1.25 kBytes, fragment size = 15 Bytes, number of pilot bits $N_P = 16$ and spreading code length $L = 16$. The probability of error conditioned on channel coefficients is averaged over 100 independent channel realizations.

Figures 8 and 9 plot the average BER and PER for various SNR values respectively. As we can see, the performance of CE-CDMA is close to the conventional DS-CDMA scheme. To archive a BER of 10^{-4} , an SNR of 20 dB and 21 dB are required with the conventional DS-CDMA and CE-CDMA schemes respectively. For a penalty of 1 dB the proposed scheme can improve the channel utilization by up to 50%. In Fig. 9, we observe that at high SNR regime the PER decreases considerably and the performance of CE-CDMA approaches even closer to the conventional DS-CDMA scheme.

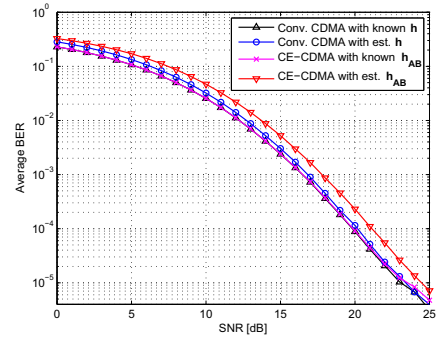


Figure 8: Average BER vs SNR. ($L = 16$, $N_P = 16$, fragment size = 125 Bytes, payload size = 1.25 kBytes).

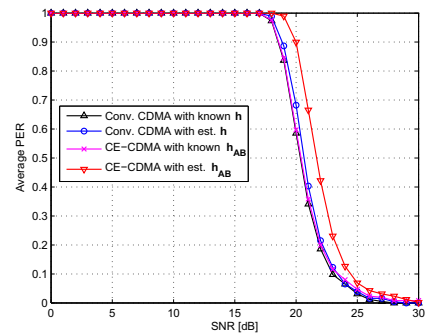


Figure 9: Average PER vs SNR. ($L = 16$, $N_P = 16$, fragment size = 125 Bytes, payload size = 1.25 kBytes).

Figures 10 and 11 plot the average BER and PER for various SNR values respectively for $N_P = 32$ instead of $N_P = 16$. We observe that the performance of CE-CDMA improves at the cost of an increase in the number of pilot bits. To achieve a BER of 10^{-4} , the CE-CDMA sacrifices less than 1dB in SNR for a potential increase in channel utilization by up to 50%. Similarly, the average PER decreases at the cost of an increase in the number of pilot bits.

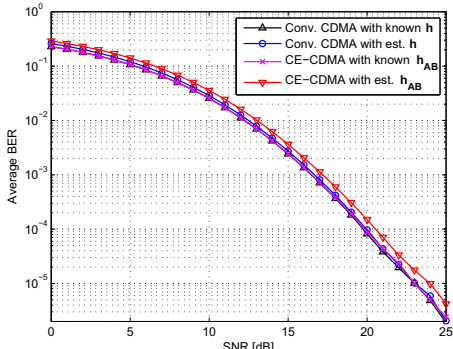


Figure 10: Average BER vs SNR. ($L = 16$, $N_P = 32$, fragment size = 125 Bytes, payload size = 1.25kBytes).

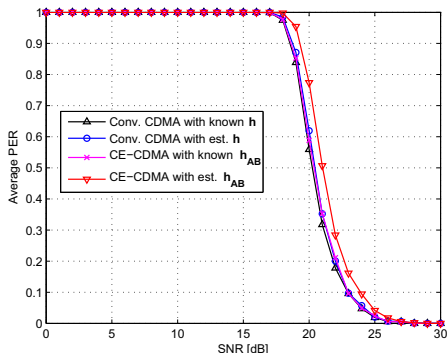


Figure 11: Average PER vs SNR. ($L = 16$, $N_P = 32$, fragment size = 125 Bytes, payload size = 1.25kBytes).

In Fig. 12, the performance of channel estimation, measured as the MSE per real channel coefficient, is shown as a function of SNR. We observe that by increasing the number of pilot bits the CSI estimation improves. Moreover, as the SNR at the receiver increases, the MSE approaches to zero.

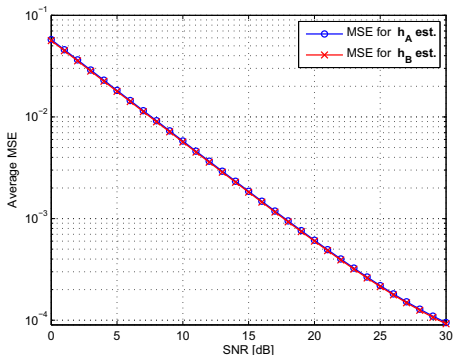


Figure 12: Average MSE of CSI estimate vs SNR. ($L = 16$, $N_P = 16$, fragment size = 125 Bytes and payload size = 1.25 kBytes).

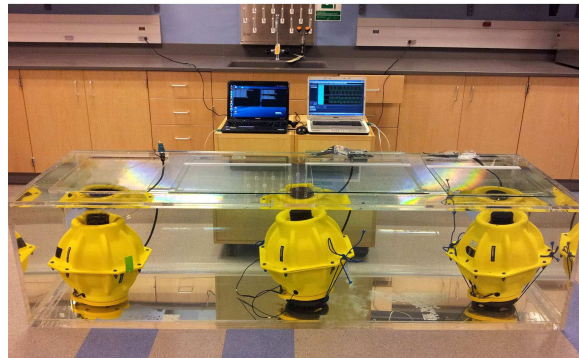


Figure 13: Experiment setup.

7.2 Experimental Evaluation

Experiments were conducted in a water tank of dimensions 8 ft \times 2.5 ft \times 2 ft in the UW-A laboratory at the State University of New York at Buffalo, using three Telesonar SM-75 SMART modems by Teledyne Benthos [1], as shown in Fig. 13. The sampling and carrier frequencies of the SM-75 SMART acoustic modem are $f_s = 10,240$ Hz and $f_c = 11,520$ Hz, respectively. The data packets were generated using Matlab, converted into a stereo WAV file in 16 bit format, and uploaded on the modems through the RS-232 interface. The DS-CDMA chip waveforms were selected from the columns of a Sylvester-Hadamard matrix of order $L = 16$. Pulse shaping was done using square-root raised-cosine with roll-off factor $\beta = 0.5$. At the chip rate $R_c = 2,048$ chips/sec, transmission data rate of 128 bit/s was generated. The modems were separated by a few feet. Initially, N_1 , located at the left corner of the tank, was selected to transmit packet P_1 to the relay node N_2 , located in the middle of the tank. In the next round nodes N_1 and N_3 transmit packets P_2 and P_1 respectively of length 1.25kBytes to the intermediate relay node, N_2 . Two computers were used to coordinate the transmissions of the packets through a serial port interface. The relay node is equipped with a data recorder that has a storage capacity of 64 GBytes. The experiments were conducted for different transmit power levels. The raw data were extracted and analyzed in Matlab. Each experiment was repeated 20 times and the average values are presented in the results.

Figure 14 shows the average BER versus SNR for payload size of 1.25 kBytes, fragment size of 125 Bytes, number of pilot bits $N_P = 16$ and $N_P = 32$. We observe that the average BER performance is slightly worse than in the simulation results due to the severe multipath effect generated by the confined walls of the water tank. We expect the performance to be better in actual shallow water environment. We can see that the performance of CE-CDMA is within a few dB from the conventional DS-CDMA scheme for a target BER. By increasing the number of pilot bits, the performance of CE-CDMA improves and approaches closer to the conventional DS-CDMA scheme.

8. CONCLUSIONS AND FUTURE WORK

In this paper, we have proposed a CE-CDMA scheme for multi-hop UW-ASNs in which two nodes utilize the same spreading code with the intention to increase the network throughput. We have developed a receiver that first jointly estimates the two multipath faded channels, then strips the

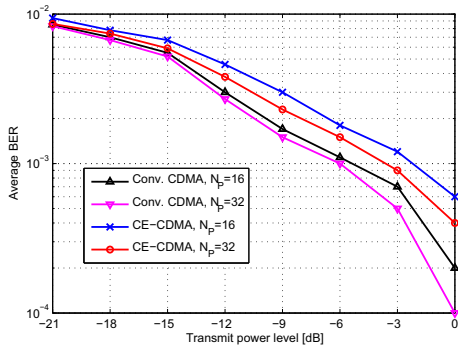


Figure 14: Average BER vs Transmit power level. ($L = 16$, $N_P = 16$ and 32 , bit rate = 128 bit/s, payload size = 1.25 kBytes).

interfered packet before decoding the information of interest. Moreover, we outline the basic functionalities of CE-MAC that supports the proposed communication scheme. We have evaluated the BER and PER performance of CE-CDMA scheme using simulations and testbed experiments. Experiments demonstrate that for a 1–2dB tradeoff in SNR the proposed scheme can improve the channel utilization by up to 50%. Our scheme will support multiple flow communication for different sessions as long as the header/trailer is decoded correctly by the relay nodes. While we have focused on transmissions by 2 nodes, in the future, we will analyze simultaneous transmissions by multiple pairs of nodes and evaluate in detail the performance of the CE-MAC protocol.

Acknowledgment

This work was partially supported by the National Science Foundation under grants CNS-1055945 and CNS-1126357.

9. REFERENCES

- [1] Teledyne-Benthos, Acoustic Modems. [Online]. Available: <http://www.benthos.com>.
- [2] I. F. Akyildiz, D. Pompili, and T. Melodia. Underwater Acoustic Sensor Networks: Research Challenges. *Ad Hoc Networks (Elsevier)*, 3(3):257–279, May 2005.
- [3] A. Argyriou and A. Pandharipande. Cooperative protocol for analog network coding in distributed wireless networks. *IEEE Transactions on Wireless Communications*, 8(10):2014–2023, October 2010.
- [4] S. Basagni, C. Petrioli, R. Petrocchia, and M. Stojanovic. Optimizing Network Performance through Packet Fragmentation in Multi-hop Underwater Communications. In *Proc. of MTS/IEEE OCEANS 2010*, pages 1–7, Sydney, Australia, May 24–27, 2010.
- [5] S. Boppana and J. M. Shea. Overlapped carrier-sense multiple access (OCSMA) in wireless ad hoc networks. *IEEE Transactions on Mobile Computing*, 8(3):369–383, March 2009.
- [6] D. L. Codiga, J. A. Rice, and P. A. Baxley. Networked Acoustic Modems for Real-Time Data Delivery from Distributed Subsurface Instruments in the Coastal Ocean: Initial System Development and Performance. *Journal of Atmospheric and Oceanic Technology*, 21(2):331–346, February 2004.
- [7] R. K. Creber, J. A. Rice, P. A. Baxley, and C. L. Fletcher. Performance of Undersea Acoustic Networking Using RTS/CTS Handshaking and ARQ Retransmission. In *Proc. of MTS/IEEE OCEANS*, pages 5–8, Honolulu, Hawaii, USA, November 2001.
- [8] M. Dankberg, M. Miller, and M. Mulligan. Self-interference cancellation for two-party relayed communication. United States Patent 5596439, January 21 1997.
- [9] A. Kansal, S. N. Batalama, and D. A. Pados. Adaptive maximum SINR RAKE filtering for DS-CDMA multipath fading channels. *IEEE Journal on Selected Areas in Communications*, 16(9):1765–1773, December 1998.
- [10] S. Katti, S. Gollakota, and D. Katabi. Embracing wireless interference: Analog network coding. In *Proc. of ACM SIGCOMM*, pages 397–408, Kyoto, Japan, August 2007.
- [11] S. Katti, H. Rahul, D. Katabi, W. H. M. Medard, and J. Crowcroft. XORs in the Air: Practical Wireless Network Coding. In *Proc. of ACM SIGCOMM*, pages 243–254, May 16–19, 2006.
- [12] H. Kulhandjian, L. Kuo, T. Melodia, D. A. Pados, and D. Green. Towards Experimental Evaluation of Software-Defined Underwater Networked Systems. In *Proc. of IEEE UComms*, Sestri Levante, Italy, September 2012.
- [13] P. Larsson, N. Johansson, and K.-E. Sunell. Coded bi-directional relaying. In *IEEE Vehicular Technology Conference (VTC) Spring*, volume 2, pages 851–855, May 7–10 2006.
- [14] B. Li, J. Huang, S. Zhou, and et al. MIMO-OFDM for high rate underwater acoustic communications. *IEEE Journal of Oceanic Engineering*, 34(4):634–644, April 2009.
- [15] T. Melodia, H. Kulhandjian, L. Kuo, and E. Demirors. *Advances in Underwater Acoustic Networking*. In Mobile Ad Hoc Networking: Cutting Edge Directions, Eds. S. Basagni, M. Conti, S. Giordano and I. Stojmenovic, John Wiley and Sons, Inc., Hoboken, NJ, 2013.
- [16] M. Molins and M. Stojanovic. Slotted FAMA: a MAC protocol for underwater acoustic networks. In *Proc. of MTS/IEEE OCEANS*, Asia Pacific, Singapore, May, 2006.
- [17] B. Peleato and M. Stojanovic. Distance Aware Collision Avoidance Protocol for Ad-Hoc Underwater Acoustic Sensor Networks. *IEEE Communication Letters*, pages 1025–1027, December 2007.
- [18] D. Pompili, T. Melodia, and I. F. Akyildiz. A CDMA-based Medium Access Control Protocol for Underwater Acoustic Sensor Networks. *IEEE Transactions on Wireless Communications*, 8(4):1899–1909, April 2009.
- [19] P. Popovski and H. Yomo. Bi-directional amplification of throughput in a wireless multi-hop network. In *IEEE Vehicular Technology Conference (VTC) Spring*, volume 2, pages 588–593, May 7–10 2006.
- [20] B. Rankov and A. Wittneben. Spectral efficient signaling for halfduplex relay channels. In *Asilomar Conference on Signals, Systems, and Computers 2005*, Pacific Grove, CA, November 2005.
- [21] B. Scheuermann, C. Lochert, and M. Mauve. Implicit hop-by-hop congestion control in wireless multihop networks. *Ad Hoc Networks (Elsevier)*, 6(2):260–286, April 2008.
- [22] E. M. Sozer, M. Stojanovic, and J. G. Proakis. Underwater Acoustic Networks. *IEEE Journal of Oceanic Engineering*, 25(1):72–83, January 2000.
- [23] B. Steiner and P. Jung. Optimum and suboptimum channel estimation for the uplink CDMA mobile radio systems with joint detection. *European Transactions on Telecommunications*, 5(1):39–50, Jan. - Feb. 1994.
- [24] M. Stojanovic. *Acoustic (Underwater) Communications*. Encyclopedia of Telecommunications, John G. Proakis, Ed., John Wiley and Sons, 2003.
- [25] M. Stojanovic and L. Freitag. Acquisition of direct-sequence spread-spectrum acoustic communication signals. In *Proc. of MTS/IEEE OCEANS*, volume 1, pages 279–286, San Diego, CA, September 2003.
- [26] M. Stojanovic and L. Freitag. Multichannel Detection for Wideband Underwater Acoustic CDMA Communications. *IEEE Journal of Oceanic Engineering*, 19:685–695, 2006.
- [27] T. C. Yang. Correlation-based decision-feedback equalizer for underwater acoustic communications. *IEEE Journal of Oceanic Engineering*, 30(4):865–880, October 2005.
- [28] S. Zhang, S. Liew, and P. Lam. Physical layer network coding. In *Proc. of ACM Intl. Conf. on Mobile Computing and Networking (MobiCom)*, pages 24–29, Los Angeles, CA, September 2006.